$M_{2,3}M_{4,5}M_{4,5}$ super-Coster-Kronig spectra of solid Ge and resonance effects around the $3p$ threshold

A. Kivimäki, H. Aksela, S. Aksela, and O.-P. Sairanen
Department of Physics, University of Oulu, SF-90570 Oulu, Finland
(Received 28 September 1992)

$M_{2,3}M_{4,5}M_{4,5}$ super-Coster-Kronig spectra of solid germanium have been measured using monochromatized synchrotron radiation. $M_2M_{4,5}M_{4,5}$ and $M_3M_{4,5}M_{4,5}$ transitions have been separated from each other. Resonance features were found at the $3p$ threshold corresponding to excitation of core excitons followed by resonant super-Coster-Kronig decay, which leaves two $3d$ holes and an excited electron in the conduction band. As opposed to normal Auger lines, these resonance features shift linearly with photon energy.

I. INTRODUCTION

When an inner shell electron is removed from an atom, the resulting electron configuration is energetically excited and the ion very rapidly moves to a lower state, e.g., by emitting an Auger electron. The goal of this work is to study Auger decay channels of $3p$ core hole states of solid germanium.

Prior to synchrotron radiation, Auger electron spectroscopy was usually practiced with electron impact or Al/Mg $K\alpha$ x-ray excitation. As far as the Auger filling of $3p$ vacancies in Ge is concerned, neither method can produce pure spectra. X-ray excitation can create vacancies up to the $2p$ level and following Auger decay cascade produces inevitably multiple hole states. Similarly, electron bombardment also creates other than singly ionized $3p^{-1}$ states. Therefore $M_{2,3}$-based Auger spectra would necessarily contain satellite transitions, if excited with electrons or Al/Mg $K\alpha$ radiation. As expected, detailed investigations of Ge Auger spectra have been made so far merely on $L_{2,3}MM$ transitions.[1–3] With synchrotron radiation, on the contrary, the excitation energy can be selected so that no shells deeper than $3p$ are reached. Following this guiding principle, we now wish to extend the analysis of Auger spectra to $M_{2,3}M_{4,5}M_{4,5}$ ($3p^{-1} \rightarrow 3d^{-2} + e^-$) super-Coster-Kronig (sCK) transitions, the strongest decay channel of the $3p$ vacant states.[4]

Resonance effects at the $3p$ threshold have been reported for several transition metals and their compounds.[5] The first observations on resonant photoemission were made from Ni by Guillot *et al.*[6] In the case of nickel and other transition metals with open $3d$ subshells, resonances can be interpreted by $3p^63d^n \rightarrow 3p^53d^{n+1}$ photoexcitation with a subsequent decay to localized $3p^63d^{n-1}$ states. These same states can also be reached by direct photoionization $3p^63d^n \rightarrow 3p^63d^{n-1} + e^-$. The interference between the two channels leads to the Fano resonance with an asymmetrical line shape for resonance intensity as a function of photon energy.[7]

The situation is more complex for Cu and Zn which have full $3d$ subshells. Nevertheless, a similar resonance has been found for both of them by Iwan and coworkers.[8,9] They explained their observations by using the atomic model: an excitation $3p \rightarrow nl$ to a quasibound state was followed by a decay to $3d^{-2}$ states with the nl electron remaining excited. Davis and Feldkamp[10] introduced a new mechanism for resonant photoemission taking into account that $3p$ electrons are not excited to a discrete level but to a band. The model was based on a strong interaction between $4s-4p$ conduction-band electrons and the $3d^8$ configuration resulting from the sCK decay of $3p$ hole states. Using this model Davis and Feldkamp were able to explain the existence of resonance in Cu and Zn. Resonant photoemission has been observed also in Ga (Ref. 11) but not in Ge to our knowledge. In this paper we present our investigations of semiconducting Ge exhibiting a resonance behavior at the $3p$ threshold.

Resonant photoemission in some other semiconductors has been known for about a decade. For example, the valence bands of silicon[12] and black phosphorus[13] have been reported to behave resonantly at the $2p$ threshold, even though the validity of these interpretations has also been questioned.[14,15] Perhaps the closest resemblance to the present case is found at the $3p$ threshold of Ga in GaP studied by Chiang and Eastman,[11] who also investigated resonant transitions to $3d^{-2}$ states.

Resonance on semiconductors can be explained by the evolution of core excitons as intermediate states at core-level thresholds.[11–13,16] Such excitons form bound states because of the strong interaction between the hole and the electron excited close to the conduction-band minimum. These core excitonic states may decay through the electron emission, where the excited electron does or does not take part in transitions, or alternatively through photon emission.[17] The electronic decay in which the electron stays excited has been called the core-exciton-induced resonant Auger process. The filling of the core hole by an outer shell electron is then accompanied by the emission of another electron while the core exciton disappears and the excited electron is transferred to the conduction band. If the excited electron participates directly to the decay being either the emitted or the core-hole filling electron, then one has a direct recombination or an autoionization process. This latter decay produces

electrons with equal kinetic energies as the direct photoemission and leads therefore to Fano-type resonance.

II. EXPERIMENT

Electron spectra following excitations of $3p$ electrons of solid Ge have been measured at MAX synchrotron radiation laboratory in Lund, Sweden. Measurements have been carried out both at the TGM beamline (BL41) equipped with a 1200 l/mm laminar grating and at the PGM beamline (BL22) having a modified SX-700-type monochromator[18] with a 1220 l/mm grating. At the TGM beamline ejected electrons were analyzed with a commercial double-pass cylindrical-mirror analyzer (CMA) applying a single channeltron detector. Most germanium spectra were recorded using a constant 30-eV pass energy which corresponds to an energy resolution of about 0.5 eV. Photon energy resolution was estimated to be 0.2–0.3 eV. At the PGM beamline a hemispherical analyzer combined to an electrostatic electron lens was used.[19] Pulse counting was accomplished by means of a multichannel plate detector system. Because of the high count rate, slit widths of only 20 μm were commonly used giving a photon energy resolution of about 0.1 eV. The contribution of the energy analyzer to total energy resolution was roughly 0.15 eV at 75-eV pass energy.

The germanium sample was prepared *in situ* by evaporating pieces of Ge attached to a tungsten filament. Tantalum and copper were used as substrate materials. The condition of the surface was confirmed by measuring photoelectron spectra of the valence band. Pressure in the vacuum chamber during measurements was about 5×10^{-10} mbar at the TGM beamline and 1×10^{-10} mbar at the PGM beamline. At the latter beamline the cleanness of the sample could be checked also by measuring spectra with high photon energy. No signals of O $1s$ and C $1s$ core lines were detected.

III. RESULTS

A. General

Figure 1 displays electron spectra of solid Ge in the kinetic-energy region from 15 eV to the $3d$ photoline. The spectra were recorded at photon energies 115, 123, and 130 eV, which are below, around, and above the $3p$ threshold. $3p$ binding energies in solid Ge are 120.8 and 124.9 eV referred to the top of the valence band.[20] All the spectra of Fig. 1 are dominated by the $3d$ photoline. Our primary concern is the kinetic-energy region 30–60 eV where there is a remarkable enhancement of intensity in the spectrum of 123 eV compared to the one of 130 eV, in which the structure is caused by $M_{2,3}M_{4,5}M_{4,5}$ sCK transitions. The 115-eV spectrum should represent a pure photoelectron spectrum in this kinetic-energy region apart from energy-loss structures of the $3d$ photoline. For solid Ge there are bulk plasmons appearing at 16.2 and about 32 eV.[21] Thus the broad structure at about 63 eV and the smaller one just below 50-eV kinetic energies in the spectrum measured at $h\nu = 115$ eV can be attributed to bulk plasmons. Also surface plasmons cause some faint structure between the $3d$ photoline and the one bulk-plasmon loss peak.[22]

In addition to the increase of intensity at ~ 45 eV kinetic energies, Fig. 1 shows the same thing also at about 20 eV. This enhancement could not be verified by the measurements done at the PGM beamline. The structure is nevertheless real and it arises from $M_{4,5}VV$ Auger transitions.[23] We may deduce that at the $3p$ threshold, where the photon energy equals the $3p$ binding energy relative to the top of the valence band, excess intensity initially occurs from transitions closely resembling the $M_{2,3}M_{4,5}M_{4,5}$ decay. Intensifying the $M_{4,5}VV$ structure, if there is any, would then come from second step processes, when the decay of $M_{2,3}$ holes has created more vacancies in the $3d$ subshell.

Let us now study more closely the kinetic-energy region between 30 and 60 eV. As an example of measurements, a spectrum recorded at $h\nu = 124$ eV is displayed in Fig. 2 where points denote experimental data and the solid line represents the estimated polynomial background. Background subtracted spectra measured at the same photon energies are added together. Some results are collected in

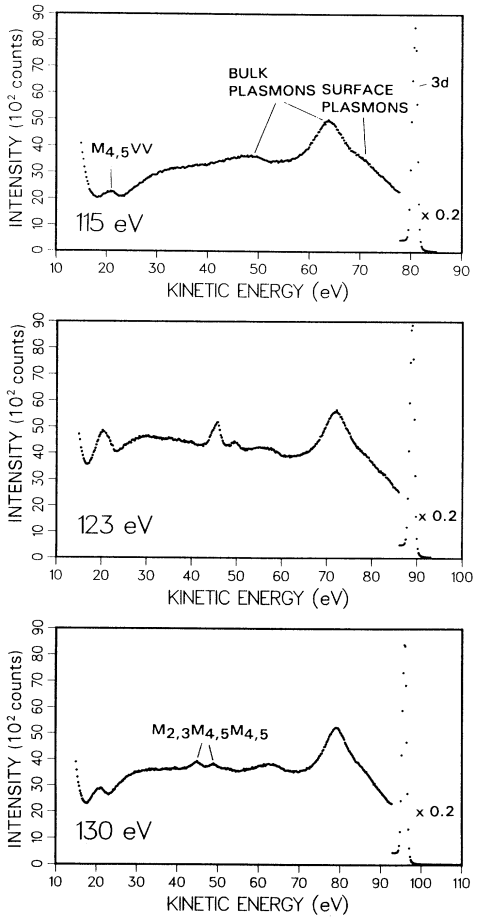

FIG. 1. Electron spectra of solid Ge at the kinetic-energy region below $3d$ photoline recorded at photon energies of 115, 123, and 130 eV.

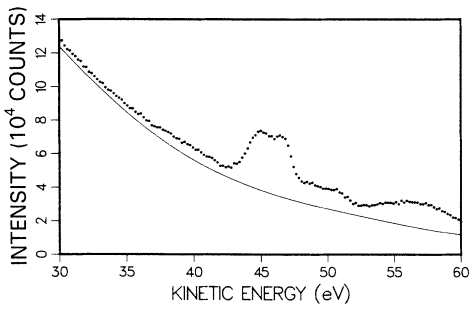

FIG. 2. An example of background subtraction. A constant background of 2×10^5 has been taken away from the spectrum measured at $h\nu$ =124 eV. The solid curve represents the estimated polynomial background to be further subtracted from experimental data depicted by points.

Fig. 3, which shows spectra recorded at photon energies ranging from 118 to 150 eV. The uppermost spectrum stands for a pure $M_{2,3}M_{4,5}M_{4,5}$ sCK spectrum with photon energy 150 eV, well above the $3p$ threshold. In all other spectra there can be seen one or two peaks that cannot arise from $M_{2,3}M_{4,5}M_{4,5}$ transitions. The extra peaks clearly follow photon energy and they are still present when the normal sCK lines disappear at photon energies below the $3p_{3/2}$ binding energy. On the other hand, since the kinetic energies of the new peaks occur at the same region as do the $M_{2,3}M_{4,5}M_{4,5}$ transitions, one can anticipate that a $3p$ hole is involved in the initial state of the process and that there are two $3d$ holes present in the final state. Most probably the rising of the new peaks comes from excitation close to the bottom of the conduction band where the electron remains more or less bound during the sCK decay. In the following this process is called resonant sCK decay.

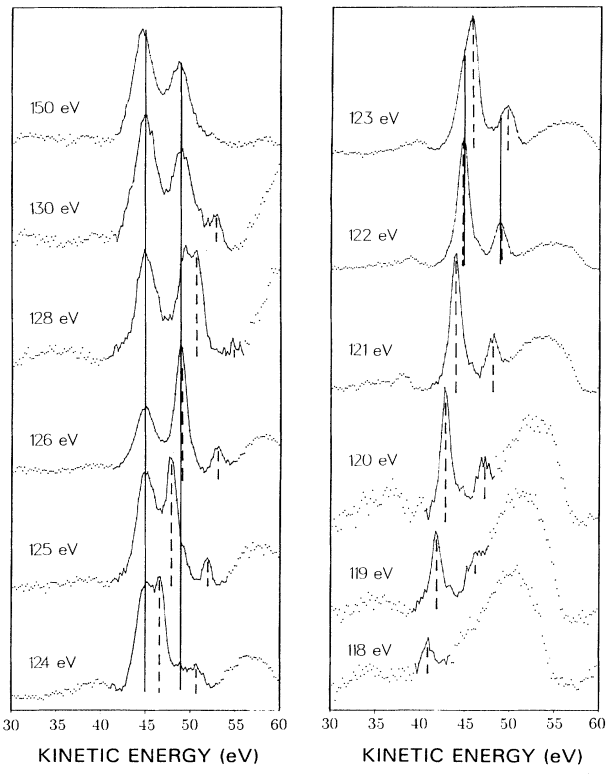

FIG. 3. Electron spectra of Ge in the kinetic-energy region 30–60 eV obtained at photon energies between 118 and 150 eV. Solid vertical bars indicate locations of the normal sCK peaks and dashed bars denote resonant sCK peaks.

B. $M_{2,3}M_{4,5}M_{4,5}$ spectrum at $h\nu$=150 eV

We postpone the excitation problem for a moment and return to the normal $M_{2,3}M_{4,5}M_{4,5}$ decay. For a comparison we have calculated a theoretical $M_{2,3}M_{4,5}M_{4,5}$ spectrum for *Ge atoms* using the multiconfiguration Dirac-Fock approach.[24,25] Statistical branching ratio of 1:2 was used for $M_2M_{4,5}M_{4,5}$ and $M_3M_{4,5}M_{4,5}$ transitions shown separately in the theoretical spectrum of Fig. 4. The sum profile is displayed by the solid line T. Linewidths used in calculated profiles are about the same as those derived from the experimental $M_{2,3}M_{4,5}M_{4,5}$ spectrum which is shown anew in Fig. 4. The overall agreement between the calculated and experimental spectra is surprisingly good bearing in mind the difference of phase. The close resemblance may indicate that these sCK transitions are

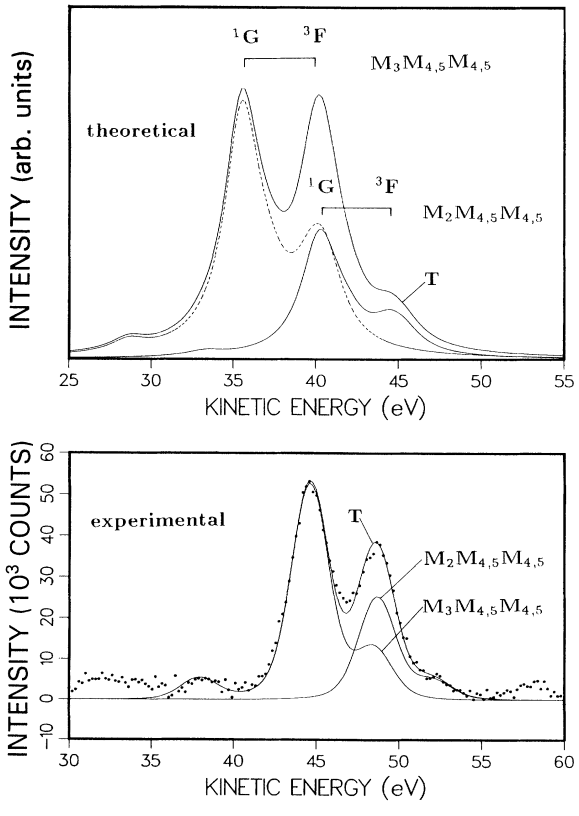

FIG. 4. Calculated atomic and experimental solid-state $M_{2,3}M_{4,5}M_{4,5}$ spectra of Ge. The decays of M_2 and M_3 holes are separated in both spectra. The main components of the decay are marked in the theoretical profile. T refers to the sum of M_2 and M_3 transitions.

essentially atomiclike in solid-state Ge, too. Calculated atomic energies differ by about 9 eV from the experimental solid-state energies. Relative energies are rather nicely produced. We may recall that LS coupling gives terms ^1S, ^1D, ^1G, ^3P, and ^3F for d^8 states, when all the other shells are closed as in Ge. The splittings between the two strongest components, ^1G and ^3F, are 3.9 and 4.7 eV in experiment and in theory, respectively. All our kinetic energies refer to vacuum level unless otherwise stated. The energies can be converted relative to the Fermi level by adding the spectrometer work function $\phi_{sp} \simeq 5.2$ eV.

The theory seems to exaggerate the ^3F peak of $M_3M_{4,5}M_{4,5}$ as well as that of $M_2M_{4,5}M_{4,5}$ decay. The former coincides with the ^1G component of $M_2M_{4,5}M_{4,5}$ decay. Hence one can suppose that also in the experimental $M_{2,3}M_{4,5}M_{4,5}$ spectrum the second peak does not rise from $M_2M_{4,5}M_{4,5}$ transitions alone. This is in fact confirmed by the spectrum measured at $h\nu = 124$ eV in which the four most intense peaks are rather well separatable and photon energy is not high enough to reach the M_2 subshell. By using the CRUNCH program code,[26] the 124-eV spectrum is in Fig. 5 decomposed to contributions coming from the normal $M_3M_{4,5}M_{4,5}$ decay and the resonant sCK decay. This spectrum also gives an

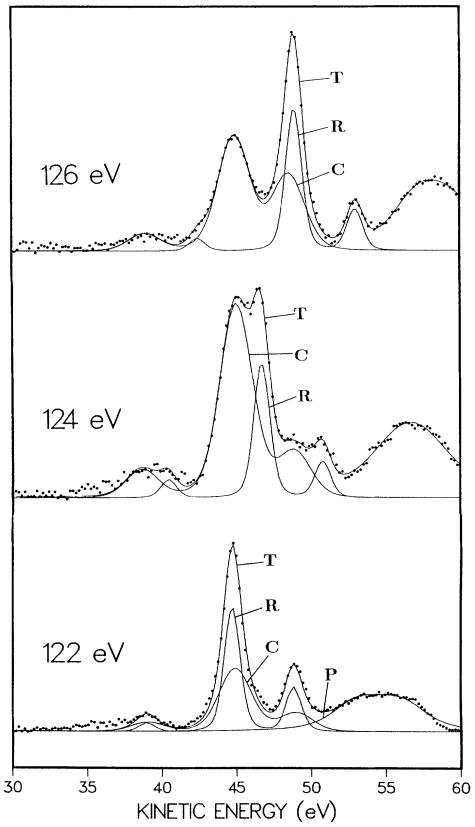

FIG. 5. Measured 122-, 124-, and 126-eV spectra decomposed to contributions originating from the normal sCK (C) and the resonant sCK (R) decay. The broad structure at the right is the two bulk-plasmon (P) loss peak of the $3d$ photoline. The sum of different profiles is given by line T.

TABLE I. Experimental kinetic energies of $M_{2,3}M_{4,5}M_{4,5}$ transitions relative to the Fermi level.

Transition		Energy (eV)
$M_3M_{4,5}M_{4,5}$	^1G	E_k=49.8±0.2 eV
$M_3M_{4,5}M_{4,5}$	^3F	E_k=53.7±0.3 eV
$M_2M_{4,5}M_{4,5}$	^1G	E_k=53.9±0.3 eV

experimental estimation for the intensity ratio between ^1G and ^3F components of the $M_3M_{4,5}M_{4,5}$ decay. The same value of ~ 0.23 can then be used to divide the 150-eV spectrum to transitions originating from M_2 and M_3 hole decay. The separation thus done yielded an experimental branching ratio M_2:M_3 of about 0.46, which is quite close to the statistical value. The results are illustrated in the experimental spectrum of Fig. 4 where the third line T shows the sum profile. The experimental kinetic energies of the three most intense components of the normal $M_{2,3}M_{4,5}M_{4,5}$ decay are listed in Table I.

The comparison between the 124- and 150-eV spectra reveals further that the ^1G component of $M_3M_{4,5}M_{4,5}$ decay shifts approximately 0.4 eV towards higher kinetic energies when photon energy is decreased from 150 to 124 eV. The change can be explained by the post-collision-interaction (PCI) effect where the parting Coster-Kronig electron is influenced by the slow photoelectron at photon energies just above the threshold. The obtained value, however, should not be taken too literally.

Recently some high-resolution studies of the surface–core-level shifts of Ge $3d$ photolines have been reported.[27,28] We do not expect to distinguish any surface contribution in our Auger spectra because Auger peaks tend to overlap even without any shift effects forming unresolved structures in solid-state spectra. Furthermore, the decay of a surface core hole can usually distribute intensity to quite a few Auger lines probably making the effect more difficult to find than in photoelectron lines.

C. Spectra of resonance region

Figure 5 represents some measured spectra separated into parts that arise from the different phenomena. For example, the 122-eV spectrum has contributions from the normal $M_3M_{4,5}M_{4,5}$ decay, from the resonant sCK decay, and from plasmons. The broad structure at the right side of the spectra is the two-bulk-plasmon loss peak of the $3d$ photoline. If we assume that its intensity does not change with photon energy in this region, it can be used as a reference for the alterations of other peaks. The plasmon is denoted by P in the 122-eV spectrum but in the other spectra the curve is not shown in order to make pictures clearer. Its inclusion in the fitting process, however, is necessary to obtain reliable results. The normal sCK transitions are depicted by the solid lines C. The intensities for different components were given approximately in the same ratio as in the 124-eV spectrum which is the only spectrum where the $M_3M_{4,5}M_{4,5}$ transitions can be rather safely separated from resonant sCK lines. Resonance contribution is denoted in the spectra by the curves R. The uppermost line T gives the sum of

TABLE II. Binding energies of the resonant sCK peaks (or $3d^8V^4C^1$ states) relative to the Fermi level.

Term	Energy (eV)
^1S	(E_b=78.0 eV)
^1G	E_b=72.2±0.3 eV
^1D	E_b=70.5±0.5 eV
^3F	E_b=68.2±0.3 eV

different contributions.

In the 122-eV spectrum resonant and normal sCK peaks occur at the same kinetic energies and their separation is somewhat problematic. It can be done, however, if the linewidths and energies are fixed. The kinetic energies of resonance lines follow faithfully the changes of photon energy while the $M_3M_{4,5}M_{4,5}$ peaks stay at fixed kinetic energies. Resonance lines are much sharper having the half-width of $\sim$ 1.2 eV compared to 2.5 eV of the sCK peaks. The width of the most intense (^1G) resonant line did not vary when measured with different photon energy resolutions. The better resolution of the lines reveals a shoulder on the high kinetic-energy side of the resonant ^1G peak. This shoulder persists there at photon energies 119–122 eV and we assign it as the ^1D term of the resonant sCK decay. The binding energies of the resonant sCK peaks are shown in Table II.

The intensity distributions of the two decays are obviously very similar. The sCK contour achieves its final form in the 126-eV spectrum. The $M_2M_{4,5}M_{4,5}$ transitions are not observed in the 125-eV spectrum (Fig. 3) although the $3p_{1/2}$ binding energy is 124.9 eV. Likewise the normal decay of the M_3 hole should already be present in the 121-eV spectrum (Fig. 3) but it is so weak that corresponding peaks cannot be extracted for certain from the experimental data. It is therefore likely that sCK decay does not occur abruptly when the $3p$ threshold is passed by but increases rather slowly.

A closer account of intensity variations as a function of photon energy is given in Fig. 6, which displays the heights of the ^1G components of the resonant sCK and

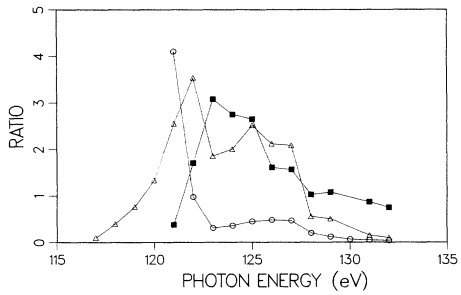

FIG. 6. Intensity variations of the normal sCK and the resonance sCK decay. Triangles: the height of the $3d^{-2}(^1G)C^1$ component of the resonant sCK decay related to the height of the plasmon structure; solid squares: the height of the ^1G component of the normal $M_3M_{4,5}M_{4,5}$ decay related to the height of the plasmon structure; circles: the probability of the resonant sCK decay with respect to the normal $M_{2,3}M_{4,5}M_{4,5}$ sCK decay calculated using the areas from zero level to fitted lines.

the normal $M_3M_{4,5}M_{4,5}$ decay related to the height of the plasmon structure. The intensity ratio between the two decays is also displayed. The last curve is obtained by using the areas from the zero level up to fitted lines and thus it gives roughly the branching ratio between the sCK and the resonant sCK decay. All points of Fig. 6 are subject to long error bars because neither the background subtraction nor the separation of the two decays can be claimed to hold true. Furthermore, the fact that measurements have been done with two different setups may cause some inaccuracy. Although the experiments were reproducible in the sense that the same peaks appear in both measurements, the spectra are not identical. For instance, the shapes of the background were ascending and descending in the spectra measured at the PGM and TGM beamline, respectively.

IV. DISCUSSION

As far as we know, no observations of core excitons at the $3p$ threshold of Ge have been reported in the literature but at the $3d$ threshold they have been mentioned by Margaritondo *et al.*[29] As it has become apparent that excitonic effects appear at all core edges of semiconductors,[30] the core-exciton-induced resonance model can be rather safely applied at the $3p$ threshold of Ge. Then the following radiationless decay channels for the core excitonic intermediate state may be considered:

$$3p^5 3d^{10} V^4 V' \rightarrow 3p^6 3d^9 V^4 + e^-, \quad (1)$$

$$3p^5 3d^{10} V^4 V' \rightarrow 3p^6 3d^{10} V^3 + e^-, \quad (2)$$

$$3p^5 3d^{10} V^4 V' \rightarrow 3p^6 3d^8 V^4 C^1 + e^-, \quad (3)$$

$$3p^5 3d^{10} V^4 V' \rightarrow 3p^6 3d^9 V^3 C^1 + e^-, \quad (4)$$

$$3p^5 3d^{10} V^4 V' \rightarrow 3p^6 3d^{10} V^2 C^1 + e^-, \quad (5)$$

where V is the valence band ($=4s^2 4p^2$ in the ground state), V' denotes the core exciton band, and C the conduction band. The first two transitions represent direct recombination and they affect the intensity of the $3d$ photolines and the valence band, respectively. The transitions (3)–(5) are different types of the core-exciton-induced resonant Auger decay. As in the case of the normal Auger decay, the $3d^8$ final states are expected to be favored. We maintain indeed that the transitions (3) cause the resonant structure easily seen in the spectra. In this context we could also speak of core-exciton-induced resonant sCK decay, since all vacancies of the process are located in the same M shell.

The close resemblance between the intensity distributions of the resonant sCK and the $M_3M_{4,5}M_{4,5}$ (or $M_2M_{4,5}M_{4,5}$) decay was already mentioned above. The shape of the resonance structure does not seem to change in any spectra unlike in the normal sCK decay. The resonant sCK structure shifts to higher energies linearly with increasing photon energy. The final states resulting from the decay of excitons are always the same. Both

spin-orbit components of $3p$ electrons are, however, involved in these processes. This can been seen from Fig. 6, where there are two maxima in the resonance emission vs photon energy curve separated approximately by the $3p$ spin-orbit splitting and corresponding to excitations of $3p_{1/2}$ and $3p_{3/2}$ electrons.

The width of the absorption energies results from the short lifetime of the core hole. There is an apparent contradiction between the broad width of absorption and the narrow resonant sCK lines. One possible explanation is that there may be also other strong decay channels besides the resonant sCK processes. The resonance peaks could also gain intensity as satellites of the direct $3d$ photoionization but this channel is negligible. Away from the resonance region the satellites were undetectable. Therefore a Fano-type resonant behavior is not expected.

The final justification of the core-exciton-induced resonant Auger model would be confirmed by the observation of all decay channels suggested by Eqs. (1)–(5). We have discovered only one of them, namely the transitions (3) which are probably the strongest. The direct recombination leading to emission of a $3d$ electron, transitions (1), would be quite difficult to observe because of the high cross section of direct photoionization at this photon energy range. Also the core-exciton-induced $M_{2,3}M_{4,5}V$ resonant Auger is probably hard to verify, since the decay is weak and overlaps with plasmons at resonant photon energies. But the remaining two decay channels (2) and (5), whose counterparts in Si and black P raised controversy, might be identifiable.

ACKNOWLEDGMENTS

We would like to acknowledge financial support from the Finnish Academy of Science. We thank T. Kaikuranta for assistance during the measurements and the staff of MAX-lab for helpful advice and assistance.

[1] J.F. McGilp and P. Weightman, J. Phys. C **9**, 3541 (1976).
[2] E. Antonides, E.C. Janse, and G.A. Sawatzky, Phys. Rev. B **15**, 1669 (1977).
[3] S. Aksela and H. Aksela, Phys. Rev. A **31**, 1540 (1985).
[4] L.I. Yin, I. Adler, T. Tsang, M.H. Chen, D.A. Ringers, and B. Crasemann, Phys. Rev. A **9**, 1070 (1974).
[5] L.C. Davis, J. Appl. Phys. **59**, R25 (1986), and references therein.
[6] C. Guillot, Y. Ballu, J. Paigné, J. Lecante, K.P. Jain, P. Thiry, R. Pinchaux, Y. Pétroff, and L.M. Falicov, Phys. Rev. Lett. **39**, 1632 (1977).
[7] R.E. Dietz, E.G. McRae, Y. Yafet, and C.W. Caldwell, Phys. Rev. Lett. **33**, 1372 (1974).
[8] M. Iwan, F.J. Himpsel, and D.E. Eastman, Phys. Rev. Lett. **43**, 1829 (1979).
[9] M. Iwan, E.E. Koch, T.C. Chiang, and F.J. Himpsel, Phys. Lett. **76A**, 177 (1980).
[10] L.C. Davis and L.A. Feldkamp, Phys. Rev. Lett. **44**, 673 (1980); Phys. Rev. B **23**, 6239 (1981).
[11] T.-C. Chiang and D.E. Eastman, Phys. Rev. B **21**, 5749 (1980).
[12] K.L. Kobayashi, H. Daimon, and Y. Murata, Phys. Rev. Lett. **50**, 1701 (1983).
[13] M. Taniguchi, S. Suga, M. Seki, H. Sakamoto, H. Kanzaki, Y. Akahama, S. Endo, S. Terada, and S. Narita, Solid State Commun. **49**, 867 (1984); M. Taniguchi, J. Ghijsen, R.L. Johnson, S. Suga, Y. Akahama, and S. Endo, Phys. Rev. B **39**, 11 160 (1989).
[14] R.A. Riedel, M. Turowski, G. Margaritondo, and P. Perfetti, Phys. Rev. Lett. **52**, 1568 (1984).
[15] T. Takahashi, H. Ohsawa, N. Gunasekara, T. Kinoshita, H. Ishii, T. Sagawa, T. Miyahara, and H. Kato, Phys. Rev. B **33**, 1485 (1986).
[16] K. Inoue, M. Kobayashi, K. Murase, M. Taniguchi, and S. Suga, Solid State Commun. **54**, 193 (1985).
[17] R.D. Carson and S.E. Schnatterly, Phys. Rev. Lett. **59**, 319 (1987).
[18] R. Nyholm, S. Svensson, J. Nordgren, and A. Flodström, Nucl. Instrum. Methods A **246**, 267 (1986).
[19] J.N. Andersen, O. Björneholm, A. Sandell, R. Nyholm, J. Forsell, L. Thånell, A. Nilsson, and N. Mårtensson, Synch. Rad. News **4** (4), 15 (1991).
[20] *Photoemission in Solids II*, edited by L. Ley and M. Cardona (Springer-Verlag, Berlin, 1979).
[21] D.L. Misell and R.A. Crick, J. Phys. C **4**, 1591 (1971).
[22] See V.Yu. Aristov, I.L. Bolotin, V.A. Grazhulis, and V.M. Zhilin, J. Electron Spectrosc. Relat. Phenom. **52**, 113 (1990).
[23] Varian chart of Auger electron energies prepared by Y.E. Strausser and J.J. Uebbing.
[24] I.P. Grant, B.J. McKenzie, P.H. Norrington, D.F. Mayers, and N.C. Pyper, Comput. Phys. Commun. **21**, 207 (1980); **21**, 233 (1980).
[25] H. Aksela, S. Aksela, J. Tulkki, G.M. Bancroft, and K.H. Tan, Phys. Rev. A **39**, 3401 (1989).
[26] C.D. Akers, C. Pathe, J.J. Barton, F.J. Grunthaner, P.J. Grunthaner, J.D. Klein, B.F. Lewis, J.M. Rayfield, R. Ritchey, R.P. Vasquez, and J.A. Wurzbach, CRUNCH *User's Manual* (California Institute of Technology, Pasadena, 1982).
[27] G. Le Lay, J. Kanski, P.O. Nilsson, U.O. Karlsson, and K. Hricovini, Phys. Rev. B **45**, 6692 (1992).
[28] R. Cao, X. Yang, J. Terry, and P. Pianetta, Phys. Rev. B **45**, 13 749 (1992).
[29] G. Margaritondo, A. Franciosi, N.G. Stoffel, and H.S. Edelman, Solid State Commun. **36**, 297 (1980).
[30] F. Bassani and M. Altarelli, in *Handbook on Synchrotron Radiation, Vol. 1*, edited by E.E. Koch (North-Holland, Amsterdam, 1983), p. 463.